Available online at www.sciencedirect.com

ScienceDirect

Ceramics International 39 (2013) 8985–8993

CERAMICS INTERNATIONAL

www.elsevier.com/locate/ceramint

# Net shape forming of green alumina via CNC machining using diamond embedded tool

Saralasrita Mohanty, Arun Prabhu Rameshbabu, Santanu Dhara*

*Biomaterials and Tissue Engineering Laboratory, School of Medical Science and Technology, Indian Institute of Technology Kharagpur, Kharagpur 721302, India*

Received 3 April 2013; received in revised form 26 April 2013; accepted 26 April 2013
Available online 15 May 2013

**Abstract**

Diamond embedded tools were fabricated through nickel electroplating of mild steel conical shaped shank for machining of green alumina compacts using Computer Numerical Control (CNC) machine. Flat and pointed end conical tools embedded with different grain sizes viz. ~117 μm (120 mesh) and ~20 μm (625 mesh) of diamond particles were used for green machining of alumina. The hardness values of 625 and 120 mesh tools were measured to be $13.79 \pm 3$ GPa and $11.84 \pm 6$ GPa, respectively. Diamond embedded tools were successfully used for net shape fabrication of symmetrical and unsymmetrical objects such as cylinder, dental crown, 3D pattern via CNC machining with submicron range surface roughness. Analysis of mechanical properties and Weibull modulus of the green and sintered alumina samples after green state machining revealed that net shape forming via green machining of alumina using diamond embedded tool is viable.


*Keywords:* Green machining; Diamond embedded tool; Weibull modulus; Net shape forming; CNC machine

## 1. Introduction

Manufacturing of complex shaped ceramic components especially medical implants like dental crowns is still a challenge, as existing direct casting techniques require fabrication of customized molds for precise size and shape [1–4]. In this respect, different mold free fabrication technologies via top-down approach may offer suitable solutions for fabrication of such customized products [5–7]. However, direct machining of bulk sintered ceramics into components is not always feasible owing to their high hardness and low fracture toughness. Machining at sintered state is not advisable mainly due to high wear rate of tool leading to impediments in removal of materials [8]. Further, any defects on the machined surface significantly reduce the strength of the finished product and additional polishing step is required to improve surface finish.

In this context, machining of green ceramics may be advantageous with the advent of recently developed net shape fabrication technologies due to relatively higher green body of ceramic compacts [9,10]. With the development of gelcasting and other coagulation casting techniques, green state machining of ceramics is emerging as a promising alternative for near net shaping [11,12]. Gelcasting was introduced by Jenny et al. and the green gelcast components are found to be sufficiently strong for green state machining, although this may involve less binder content [13,14]. The pioneering work of green state machining of gelcast ceramics was reported by Nunn et al. in the mid 90's [15]. Green state machining of ceramics is an energy efficient process for preparation of net shape components and allows reduction of surface defects for notches associated with green machining during densification.

Further, Kamboj et al. have reported machining of green gelcast ceramics and their bisque fired components via grinding, milling and drilling [16]. From this study, it was evident that both milling and drilling of gelcast alumina were made difficult due to high wear rate of High Speed Steel (HSS) tool employed in the process. Similarly, though, grinding operation

*Corresponding author. Tel.: +91 3222282306.
*E-mail address:* sdhara@smst.iitkgp.ernet.in (S. Dhara).

0272-8842/$ - see front matter © 2013 Elsevier Ltd and Techna Group S.r.l. All rights reserved.
http://dx.doi.org/10.1016/j.ceramint.2013.04.099

was feasible using porous SiC wheel it required frequent dressing to avoid clogging of the grinding wheel. This study concluded that alternative wear resistant tool materials and design would be necessary for machining of ceramics based on grinding and milling.

Dhara et al. have studied efficacy of HSS, carbide and diamond coated tools on differently processed green ceramics [9]. They reported that green body prepared by Protein Coagulation Casting (PCC) was difficult to machine using HSS and carbide coated tools due to high tool wear rate. It was observed that that diamond coated tools yielded superior machining performance due to their high hardness and abrasiveness. However, tool geometry played an important role for rate of materials removal, surface finish and creation of complex curvatures. Diamond coated flat-end tools offered effective machining with good surface finish of the green ceramic compacts in comparison to the rounded tools [9]. It was also noted that good edge retention could be achieved by controlling the chip size during machining. Indeed, smaller chip size is preferable during machining of brittle materials for better edge retention and surface finish. Using diamond coated tools, Su et al. machined different complex shaped ceramic objects viz. micro channels, molar teeth and scaffolds via machining approach [11]. In their study, 0.5 mm diameter diamond coated end mill was used to achieve complex curvatures with good surface finish in fabrication of micro channels. However, the difficulty in machining operation was associated with poor stability of the tool. Furthermore, green machining of ceramics is not yet popular due to limited availability of the diamond coated tools.

In the present context, metal-bonded diamond impregnated tool is emerging for wide varieties of applications viz. sawing, drilling, cutting, grinding, polishing of rocks, concrete and ceramics [17–19]. The tool consists of diamond particles embedded randomly within a metallic matrix through different bonding methods viz. metallic/resin bonding, electroplating, and vitrification. This tool is relatively cost effective and offers long life due to its high hardness and abrasion resistance. Oliveira et al. [20] fabricated metal-bonded diamond embedded tool via powder metallurgy route for marble cuttings using Fe–Cu–SiC as a metal matrix. The selections of bonding materials are normally considered on the basis of the hardness and wear resistance properties of the work piece material to be machined. Generally, tungsten, copper, cobalt, nickel, iron, iron–cobalt alloys, iron–nickel alloys etc. are used as bonding metals for development of diamond impregnated cutting tools [21,22]. Interestingly use of such tools for net shape fabrication of green ceramics via CNC machining is not yet reported.

In the present study, super abrasive diamond embedded tools based on electroplating of nickel on mild steel shank are developed with customized tool design for net shape fabrication of alumina components via green machining. As part of the tool development, tool geometry and tool materials were considered to be important for removal of materials based on grinding and milling. Machinability of green alumina using this novel tool was tested on the green compacts prepared by PCC for customized products. Microstructure and mechanical properties (flexural strength and hardness) of the green and sintered polished samples were compared with machined samples (green and sintered) to assess the efficacy of the process.

## 2. Experimental procedure

### 2.1. Designing and manufacturing of tool

For designing of tools for green state machining, different parameters like size, shape, and surface architecture of the components were taken into consideration. Further, tool stability was also customized into the design based on prior experience of green machining. For net shape fabrication of alumina based green compacts via green state machining, diamond particles were selected to be embedded onto metallic shank to improve the wear resistance property of the tool during operation. These diamond particles provide rough surfaces for scooping out of materials and protect the tools from wearing out. Cylindrical tools with conical flat and pointed end tip were designed to impart stability during machining of fine features.

Based on the above scheme, primarily the mild steel cylindrical shank (~3 mm diameter) with conical tip (surface angle of 10°) was inserted into an electroplating chamber as per the designs (Fig. 1(a) and (b)) for electro-bonding of diamond particles. Owing to high hardness and wear resistance property, nickel was chosen as metal matrix for diamond embedding. Electroplated diamond tools were manufactured through the bonding of specified grit diamonds by the process of electrolysis. Diamond particles were randomly distributed

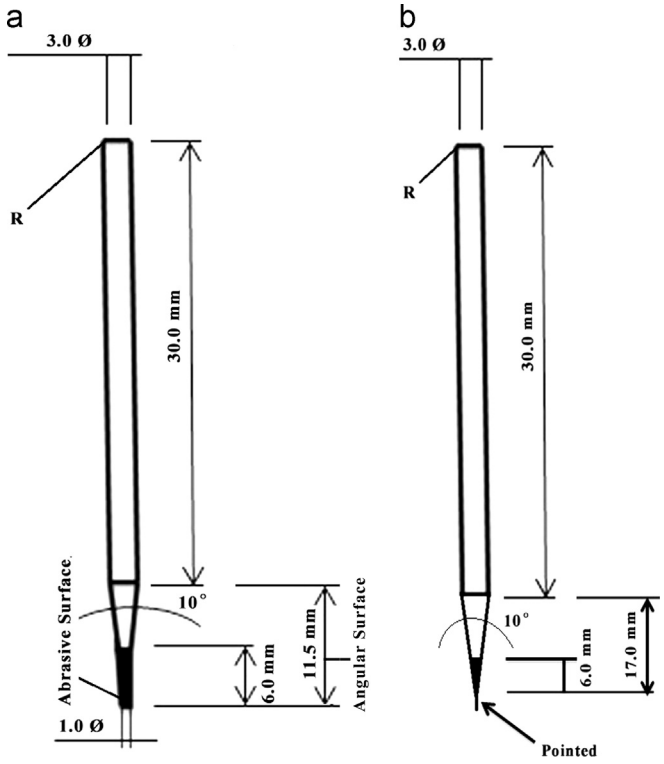


Fig. 1. Schematics of (a) conical flat end and (b) conical pointed end tool.

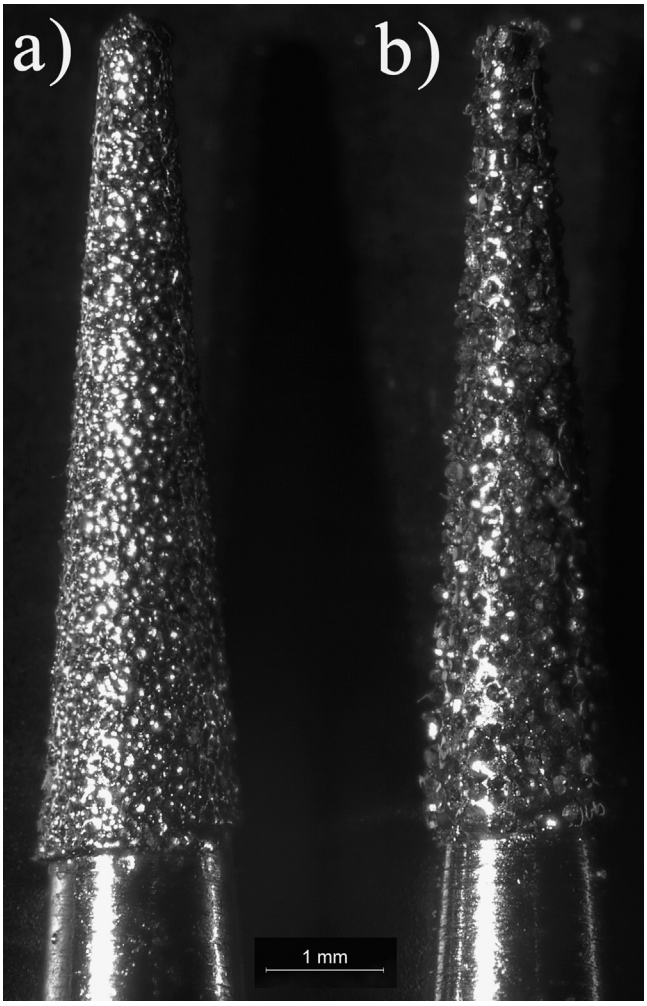


Fig. 2. Optical images of diamond embedded (a) 625 mesh and (b) 120 mesh tool.

over the steel body. This body acted as the cathode in the electrolytic circuit. Highly pure nickel plate was used as the anode. Nickel sulfate and nickel carbonate combined with saccharine, boric acid and sodium laurel sulfate were used as the electrolysis bath following the procedure developed by Li et al. [23]. When current was applied, nickel was deposited on steel base and built up to a level around the scattered diamond particles lying on the shank and facilitated gripping of the diamond particles on the shank. Thus, the electro-bonding of the diamond was completed. The grain size of the diamond particles were selected based on initial experiments. Following the above mentioned procedure, two different grain size diamond particles viz. 120 mesh (~117 μm) and 625 mesh (~20 μm) were considered for embedding on tool surface and accordingly named as either 120 mesh tool or 625 mesh tool, respectively. Optical images of the fabricated conical pointed end tools are shown in Fig. 2a and b.

### 2.2. Characterization of machining tool

Hardness of the 120 and 625 mesh tools was measured by Vickers's indentor (Model: UHL-VMHT, Germany) using 300 g force with 15 s dwell time. Tools were inspected under Scanning Electron Microscope (SEM, EVO60/Zeiss, Germany) in order to investigate surface morphology before and after green machining of ceramics. To analyze the effect of tool wear during machining, weight loss of duly cleaned tools was measured after machining for 16 h and a comparison was made between 120 mesh and 625 mesh tools. Quantitative analysis of number density and percent area covered by embedded diamond particles were measured using SEM images by image analysis software (Image Tool, Version 3.0, University of Texas, Health Science Center, Antonio) and compared their performances after machining for 16 h.

### 2.3. Preparation of green alumina compacts

Alumina powder (RG 4000, Almatis, Germany) was used for preparation of machinable green ceramic compacts. Highly loaded aqueous alumina slurries were prepared using polymaleic acid (PMA, Aquapharm, India) as dispersant [18]. Based on prior optimization study, PMA concentration of 3.8 mg per gram of alumina powder at pH 9 was used as the optimum concentration for preparation of highly loaded aqueous alumina slurry (55 vol%). Mixture of ovalbumin and sugar was used as a binder for coagulation of slurry into gel. The amount of binders in the final slurry were optimized through rheological study. Finally, 55 vol% alumina loaded slurry was prepared by adding 10 vol% ovalbumin, 3 wt% sucrose (on ceramic powder weight basis) and zirconia ball (3 mm average diameter, Zirconox, Jyoti Ceramics, India) as milling media. After 24 h of milling, the slurry was homogeneous with good flow ability. The milling media was removed from slurry through sieving followed by addition of 1-octanol as antifoaming agent (Merck, India, 1 ml/100 ml of slurry). Further, slurry was rolled for 1 h at low rpm which allowed the bubbles to escape [24]. Antifoaming agent may also be added just after addition of binder and slurry may be centrifuged to remove the air bubbles as per the necessity. Different rectangular and cylindrical silicon rubber molds were used for casting of the de-aired slurry. Prior to casting, all the molds were coated with white petroleum jelly. Bubble free slurry was cast into the molds and dried at 40 °C under controlled humidity to avoid warpage associated with drying. The dried alumina samples were removed from the mold and stored for net shape forming via machining. Also, the dried samples were subjected to binder burnt out and sintered in a chamber furnace (Bysakh, Kolkata, India) at 1550 °C for 2 h at a heating rate of 2 °C/min.

### 2.4. Characterization of green and sintered alumina body

Bulk green and sintered density of alumina compacts was measured by the Archimedes method [25]. Micro-hardness measurements of green alumina compacts were carried out using a Vicker's diamond indenter (Model: UHL-VMHT, Germany) operated at a load of 5 g force with an indentation dwell time of 10 s. Further, for measurement of micro-hardness of sintered samples, LECO Hardness Tester (LV 700, LECO

Corporation, USA) was used under 1000 kgf load with 10 s dwell time. Prior to hardness measurement, all the samples were polished and coated with black ink to focus under optical microscope. At least five indentations were taken at different positions of the samples for each specimen and the average values were reported. Both green and sintered bodies were characterized for their mechanical properties and microstructure by SEM. For SEM, the samples were gold coated (Polaron sputter coater, GmbH, UK) for 1 min prior to analysis. Microstructures of machined alumina samples surfaces at green and sintered state were examined at an accelerating voltage of 10–20 KV.

### 2.5. Machining operation

Green machining operation was performed by a bench-top CNC milling machine (MDX 540, Roland DG Ltd., Japan) using conical flat end and pointed end diamond embedded tools with different mesh sizes (120 mesh and 625 mesh) to evaluate the machining efficacy of tool material and tool geometries on the surface finish of machined alumina. Prior to machining, vacuum dried green alumina samples were mounted on the table of CNC machine. Surfacing and net shape forming of green alumina compacts were attempted via green state machining using diamond embedded tools and their machinability was compared for surface finishing, tool life and influence of surface quality on mechanical properties.

Prior to machining, 'stl' format of 3D image of a cylinder was created to fabricate alumina compacts via direct machining. The tool was mounted on the CNC machine and alumina cylinder was fabricated by green machining as per the 3D design. Based on the mechanical properties and green density of the alumina compacts, the machining parameters like depth of cut, rpm, rate of movement of tool and distance between tool paths were optimized during surfacing/roughing and the final components were attempted to be fabricated at least possible time using the optimized machining parameters. The optimum machining parameters are shown in Table 1. Further, to investigate the viability of this machining process using the diamond embedded tools for development of customized or asymmetrical objects. Human tooth (incisor) was also attempted. Micro machining capability was also evaluated using pointed end tool.

### 2.6. Characterization of machined surface

Quality of machined surface was assessed by stereozoom optical microscopy (MVX 10, Leica, Germany), SEM and surface profilometry (Talysurf i60/i120/i200-Inductive Systems, Taylor Hobson Limited, Leicester, England). Arithmetic mean roughness ($R_a$) was measured by surface profilometer at 1 mm interval of each sample along and perpendicular direction of machining using contact type stylus profilometer with a 1 μm tip radius. The flexural strength of machined sintered and sintered polished alumina samples were measured and compared with sintered polished samples, in order to evaluate the influence of machining parameters on the mechanical properties. For flexural strength measurements, rectangular size alumina samples with dimensions of 40 mm × 5 mm × 3 mm by length, breadth and thickness, respectively, were used. Prior to the strength measurement, green rectangular bars were machined (via surfacing and finishing) perpendicular to the length of the bar and placed in the furnace for sintering at 1550 °C for 2 h. The flexural strength of both machined sintered and sintered polished rectangular alumina samples were measured at room temperature (25 °C) using three point bend test fixture (ASTM D790 test standard). The bend test was performed by a universal testing machine (Model: HEK25, Hounsfield, UK) at cross head speed of 0.5 mm/min using 5000 N load cell with a span of 25 mm. Weibull modulus [26,27,28]of the sintered polished and machined sintered rectangular samples (ten data points) were calculated for reliability.

## 3. Results and discussion

Diamond embedded tools were manufactured via electroplating of nickel on mild steel conical shaped shank for machining of green alumina compacts. Microscopy (optical and SEM) analyses revealed that diamond particles were embedded partially on the electroplated Ni surface (Fig. 3(a) and (b)). From the image analysis software, it was observed that diamond particles covered ~50% and ~58% of the area for 625 mesh tool and 120 mesh tool, respectively. Further, the number density of diamond particles embedded on the 625 mesh tool and 120 mesh tool were found to be 320/mm$^2$ and 56/mm$^2$, respectively. The projection of diamond crystals was more prominent in case of 120 mesh tool compared to that of the 625 mesh tool. The exposed diamond crystals on the tool surface were beneficial for removal of the materials from the green body and surface finish of the green alumina was dependent on size of the diamond particles. From SEM microscopy, it was revealed that the deposition of smaller diamond particles (~20 μm) was more uniform in comparison to coarse particles (~117 μm). The average hardness values of

Table 1
Optimized machining parameters during green machining of alumina compacts.

| | Surfacing | Roughing | Finishing |
|---|---|---|---|
| XY Speed (mm/s) | 10 | 10 | 8 |
| Z Speed (mm/s) | 5 | 5 | 4 |
| Spindle rpm | 10,000 | 10,000 | 10,000 |
| Depth of cut (mm) | 0.5 | 0.5 | 0.2 |
| Path interval (mm) | 0.1 | 0.1 | 0.1 |

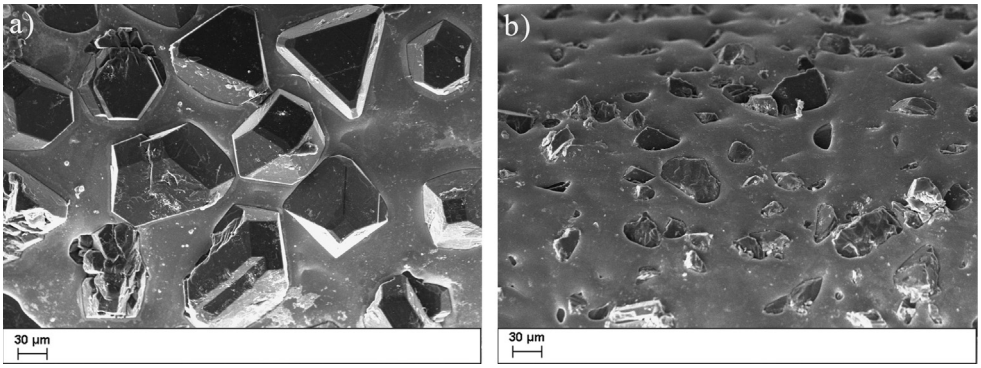


Fig. 3. SEM microstructures of (a) 120 mesh tool and (b) 625 mesh tool.

the tools were $13.79 \pm 3$ GPa, $11.84 \pm 6$ GPa for 625 mesh and 120 mesh, respectively. However, there was a wide distribution of hardness values for 120 mesh which could be attributed to uneven distribution of relatively bigger diamond particles on the shank surface. The hardness value of nickel deposited mild steel in absence of diamond particles was $6.67 \pm 3$ GPa.

The highly loaded alumina slurry (55 vol%) used for preparation of green compacts had viscosity of 4.7 Pa s at shear rate 5.6 $s^{-1}$. The green density of dried alumina compact was 63% of the theoretical density was satisfactory for achieving sintered density of more than 98%. The alumina green body contains about 4 wt% binder with hardness of $0.41 \pm 3$ GPa. Average linear shrinkage due to drying of the alumina samples was measured to be ~2%. The fracture surfaces of vacuum dried and sintered samples had negligible defects/bubbles as investigated by SEM. The flexural strength and compressive strength of green alumina samples were measured to be $10.2 \pm 4$ MPa and $19.5 \pm 2$ MPa, respectively.

Initially, surfacing of the green alumina was successfully carried out by diamond embedded tool at a speed of 10 mm/s along *X*, *Y* axis and 5 mm/s along *Z* axis with tool rpm of 10,000. Prior surfacing study of the green alumina compacts by carbide coated tools revealed that there was a black mark along the tool path after ~10 min of machining due to scrubbing of the metal shank with samples related to wearing out of the carbide coating [9]. However, no such black mark appeared along the tool path on the machined surface during green machining by the diamond embedded tool for about 16 h and machined surface exhibited good surface finish.

Besides surfacing, green machining capability of bulk alumina compacts were also tested by this tool for net shape forming using CNC machine. It was revealed that the optimization of different machining parameters like *X*, *Y* and *Z* speed of tool movement, tool rpm, depth of cut, tool path interval, and direction of machining were important for efficient materials removal rate and quality surface finish. Using the optimized parameters as given in Table 1, different symmetrical and asymmetrical objects were fabricated by this process without use of any coolant. In this study, tool movements at *X*, *Y* speed of 10 mm/s in *X*, *Y* direction and *Z* speed of 5 mm/s at *Z* direction and 10,000 tool rpm were used successfully for machining of bulk components. Similar study of green machining using diamond coated end mill by Dhara et al. has reported linear tool movements as *X*–*Y*–*Z* speed of 14 mm/s and 14,000 tool rpm [9]. It is noteworthy that relatively less linear *Z* speed (5 mm/s) and less depth of cut were essential for net shape forming, as the diamond embedded tool did not have helical flute feature on the cutting surface for easy removal of chips during machining operation.

For net shape fabrication, the green alumina compacts were machined by three steps viz. surfacing, roughing and finishing. The tools performed efficiently for prolonged period of time during machining of green alumina compacts. Clogging of the particles on the tool surface was insignificant and the clogged particles could not hamper the machining even after long periods of operation. Actually, the embedded diamond particles on the surface of the conical shaped bonded matrix offered a rough surface which eventually facilitated scooping out of the materials effectively through milling/grinding.

The 120 mesh tool offered higher materials removal rate owing to high surface roughness associated with bigger diamond particles in comparison to the 625 mesh tool. However, both the tools pursued similar materials removal rate due to identical machining parameters. The flat end tool could be used with higher path interval in comparison to conical end tool and facilitated faster removal rate of materials. However, fine features were more prominent with conical end tool in comparison to that of the flat end tool. Thus, flat end 120 mesh tool could be used for surfacing and roughing along with conical end 625 mesh tool for finishing of linear symmetrical objects effectively. Whereas, conical pointed end 120 and 625 mesh tools could be efficiently used for roughing and finishing of fine features with complex shapes, respectively. Symmetrical and unsymmetrical net shapes like cylinder and dental crown were fabricated successfully using diamond embedded tool as shown in Fig. 4a and c. Further, micro-pattern on the green alumina was also fabricated with good edge retention using conical pointed end 625 mesh tool (Fig. 4 (b)). Optical microscopy revealed that the machined surface of green alumina for 120 and 625 mesh tools had surface roughness owing to removal of materials by the diamond embedded tools (Fig. 5(a) and (d)). From the SEM of the sintered samples, it was observed that the tool movement mark was more prominent for 120 mesh tool in comparison to that of the 625 mesh tool (Fig. 5 (b) and (e)).

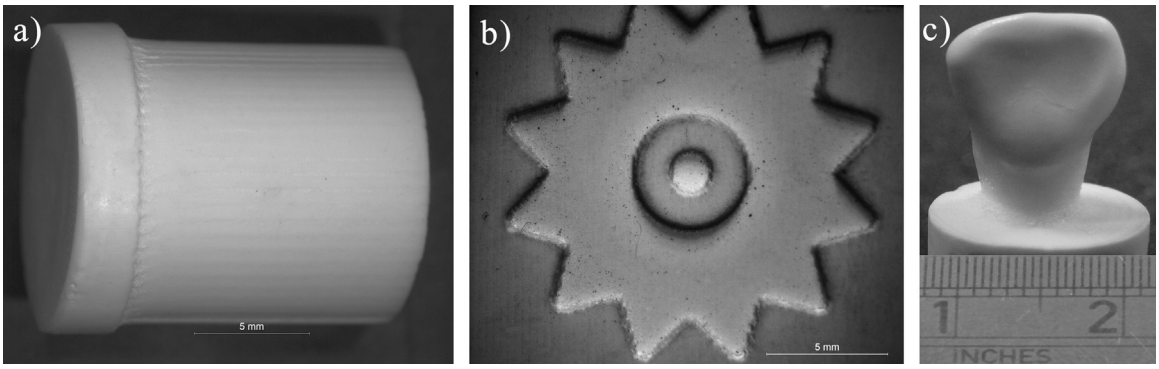


Fig. 4. Optical images of (a) cylinder, (b) 3D micro-pattern, and (c) dental crown (Incisor) fabricated by green machining using diamond embedded conical pointed end tool.

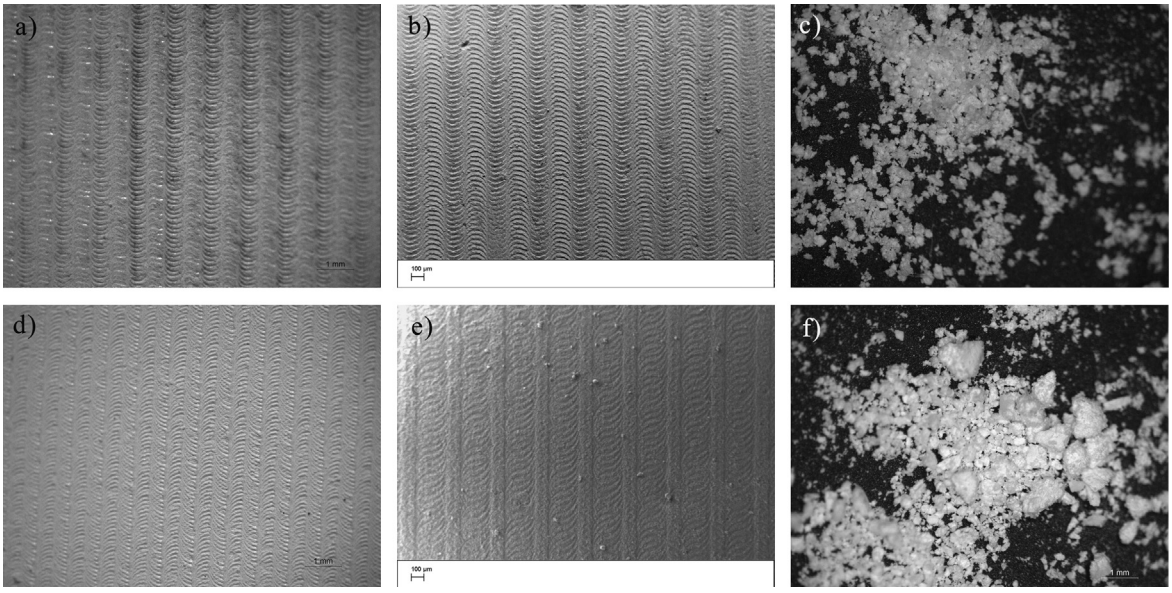


Fig. 5. (a) Optical image, (b) SEM micrograph of machined alumina surfaces, (c) chips produced using 120 mesh conical pointed end tool, (d) optical image, (e) SEM micrograph of machined alumina surfaces, and (f) chips produced using 625 mesh conical pointed end tool during green state machining of alumina samples, respectively.

SEM microscopy of the bisque fired sample revealed particles arrangement along the tool path during machining and grain growth after sintering as shown in Fig. 6a and b, respectively. The surface roughness created by 120 mesh tool was higher than that of the 625 mesh tool (Fig. 7 (a) and (b)) according to the size of the embedded diamond particles.

The surface profile of the machined green and sintered samples along and perpendicular directions to the tool path were measured. The average surface roughness of the sintered samples along the tool path was in the submicron range ($\sim 0.19 \pm 0.06$ μm and $0.10 \pm 0.03$ μm for 120 and 625 mesh tools, respectively) with random spikes created by tool movement. However, the surface roughness perpendicular to the tool path was relatively higher (average roughness $0.82 \pm 0.03$ μm) with presence of spikes of ~2 μm peak at regular interval of 0.2 mm associated with tool path interval for 120 mesh tool (Fig. 7(a)). For 625 mesh tool, the average surface roughness was relatively less ($0.42 \pm 0.04$ μm) and the spikes were relatively less regular with average peak of ~1 μm associated with tool path and surface roughness (Fig. 7(b)). The spikes and arithmetic average roughness of the machined samples were less prominent after sintering associated with shrinkage using both the tools (Table 2, Fig. 8 (b) and (e)). The average roughness of the sintered samples were about $0.59 \pm 0.08$ μm and $0.2 \pm 0.06$ μm in case of 120 and 625 mesh tools, respectively (Table 2, Fig. 7 (c) and (d)). It is noteworthy that the surface smoothness of all the samples was in the submicron range and was similar to the surface roughness (~0.3 μm) reported by Dhara et al. [9] using diamond coated 0.5 mm diameter end mill. Further, chip size of the machined samples using these tools, as observed by optical microscopy, was powder like and relatively coarser powder was produced by 120 mesh tool in comparison to 625 mesh tool (Fig. 6(c) and (f)). As the chip size was much finer than the conventional end milling procedure, the surface was less sensitive to irregular fracture and had good surface finish.

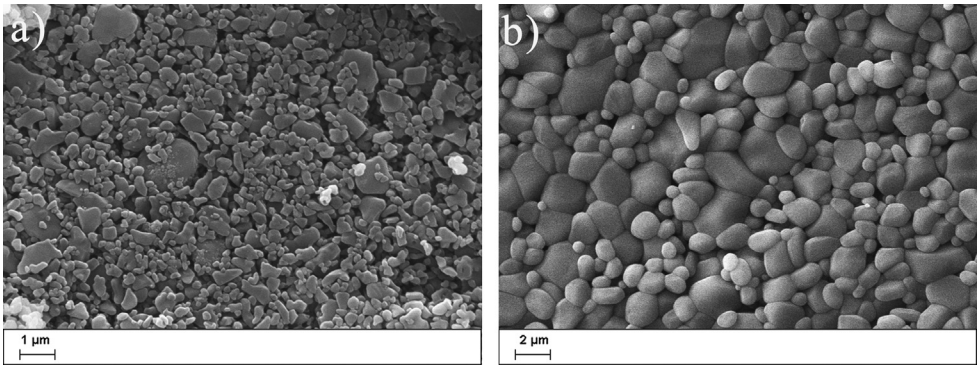


Fig. 6. SEM microstructures of the machined alumina samples after (a) bisque firing and (b) sintering.

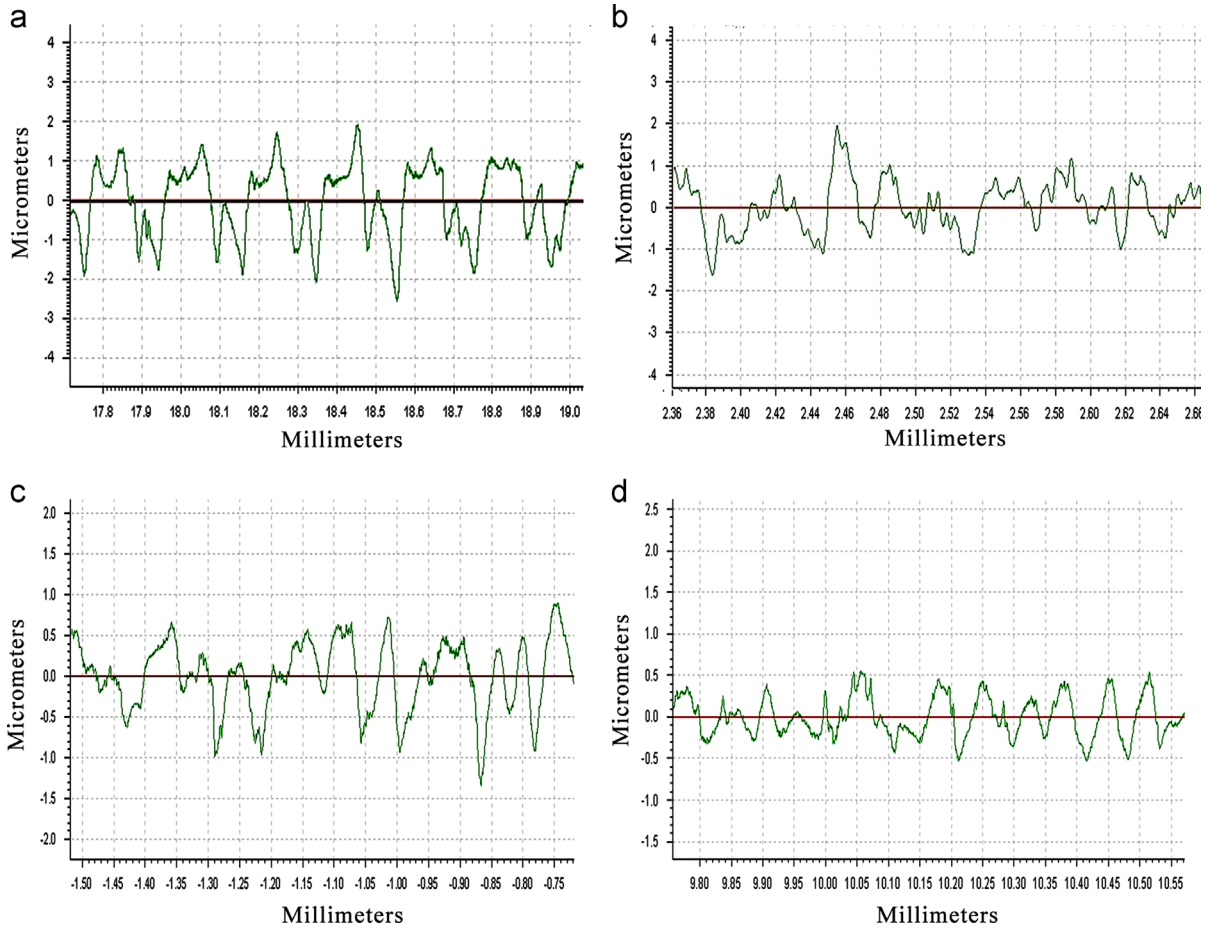


Fig. 7. Surface profile along the perpendicular direction of the machined samples produced using conical pointed end tool (a) machined green, (b) machined sintered samples by 120 mesh tool, (c) machined green, and (d) machined sintered samples by 625 mesh tool, respectively.

However, materials removal rate using these tools were relatively less and provided better edge retention which was beneficial for micro patterning.

The wear rate of the tools was determined by tool weight loss measurement at different time intervals during machining. Insignificant tool weight loss ( $< 1$ wt%) was recorded after removal of 19 ml of materials in 16 h from green alumina compacts under optimized machining parameters using diamond embedded tools. Even with similar materials removal rate obtained with both the tool types, wear rate was comparatively less for 625 mesh tool owing to smaller grain size and higher number density of the embedded diamond particles. The abrasion resistance and the stability of the 120 mesh tool was relatively less in comparison to 625 mesh tool even with marginally higher surface coverage mainly due to more diamond granules pull out from the bonded metal matrix during machining as shown in Fig. 8a and b. However, such pull out of diamond particles was insignificant in case of 625 mesh tool which is due to the impregnation of smaller diamond particles on the metal bonded matrix. This facilitated higher

Table 2
Surface roughness data of the machined surface using diamond embedded conical pointed end tool.

| Tool type (Diamond mesh size) | Average surface roughness (μm) | | |
|---|---|---|---|
| | Perpendicular to tool path | | Along tool path |
| | Green | Sintered | Sintered |
| 120 mesh | 0.82 ± 0.03 | 0.59 ± 0.08 | 0.19 ± 0.06 |
| 625 mesh | 0.42 ± 0.04 | 0.20 ± 0.06 | 0.10 ± 0.03 |

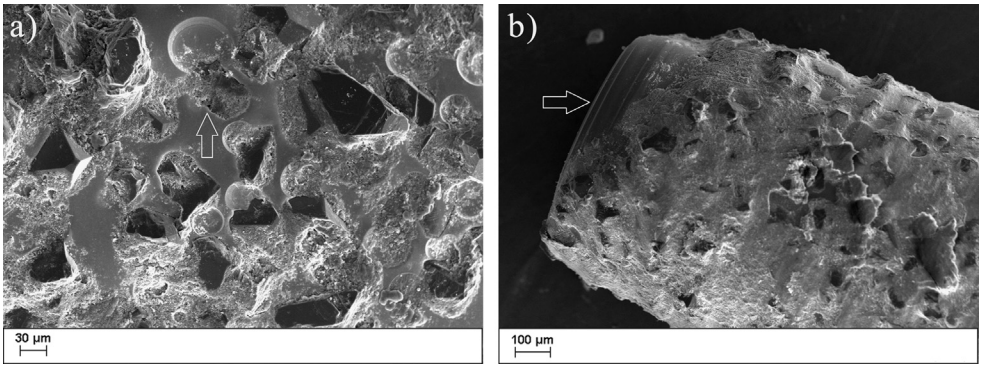


Fig. 8. SEM micrograph of diamond embedded tool after machining (a) arrow indicating the pull-out of diamond crystals during machining and (b) arrow indicating wear out of diamond granules and electroplated nickel from the shank.

abrasion resistance and hence offered better tool life compared to 120 mesh tool.

The hardness of the sintered alumina compacts was measured to be 21 ± 0.5 GPa. The average three-point bending strength of both machined and sintered polished alumina (using 120 mesh and 625 mesh tools) were measured and compared with sintered polished samples. The average flexural strength of machined sintered samples by 120 mesh tool showed relatively lower value (289 ± 33 MPa) followed by 625 mesh tool (319 ± 28 MPa) than the sintered polished alumina samples (345 ± 27 MPa). This indicates that the average surface roughness generated during green machining using different mesh size diamond embedded tools has certain influence on flexural strength even after reduction of roughness associated with shrinkage during sintering.

The influence of the green machining on the reliability of final sintered alumina components was studied using Weibull statistical tool. Weibull plot of bend strength distributions of the machined sintered and sintered polished alumina samples (10 each) are shown in Fig. 9. From the Weibull plot, it is verified that modulus values ($m$) are greater than 5 with similar regression coefficient for the samples. There was no such significant difference in Weibull modulus ($m$) value for sintered polished alumina sample (11.8) and machined sintered alumina sample using 625 mesh tool (10.8). However, relatively less '$m$' value (8.2) was obtained for 120 mesh machined sample. This difference in Weibull modulus and average flexural strength were associated with surface roughness produced during green machining of alumina compacts using higher mesh size diamond embedded tool. Whereas, relatively less Weibull modulus value ($m$=5.2) was reported

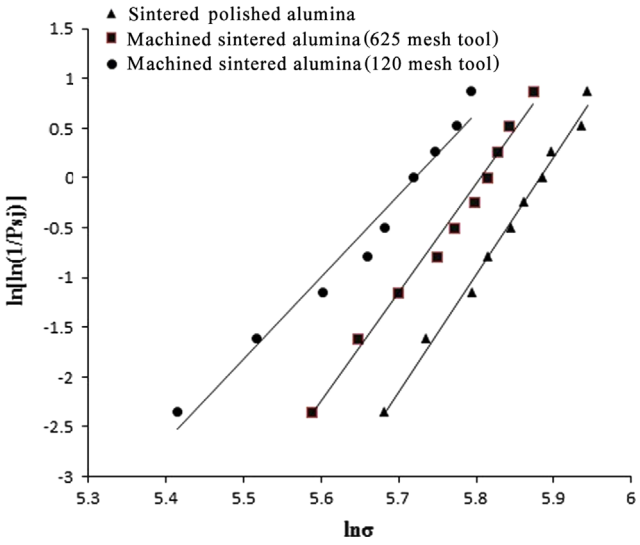


Fig. 9. Weibull modulus plot of sintered PCC alumina ceramics with sintered polished and machined sintered using 120 and 625 mesh diamond embedded tools, respectively.

by Su et al. for machining of green alumina using diamond coated end mill [11]. Thus, edge retention, controlling chip size and average surface roughness are important during machining of brittle samples which ultimately depended on tool geometry and tool surface feature.

## 4. Conclusion

Different customized diamond embedded tools were successfully designed and manufactured through electroplating of

nickel on the surface of mild steel conical shaped shank for green machining of alumina compacts. The conical flat end and pointed end diamond embedded tools with different grain sizes ~117 μm and ~20 μm of diamond particles were used for net shape fabrication of green alumina compacts via CNC machining. The machining behavior of the tools was found to be influenced by tool materials, tool geometry and optimized machining parameters. The conical flat end 120 mesh tool could be used for surfacing/roughing, whereas conical pointed end 625 mesh tool could be used for finishing of linear symmetrical objects. Conical pointed end tool could be efficiently used for roughing and finishing of fine features with complex shapes. Dental crown, 3D pattern, cylindrical bar were successfully fabricated via green machining using diamond embedded pointed end tools. The wear rate of 625 mesh tool during green state machining operation was relatively less compared to 120 mesh tool. The machined green alumina had good quality surface finish with roughness in the submicron range. From the Weibull modulus values of the machined sintered alumina, it could be concluded that net shape forming via green state CNC machining using diamond embedded tool is a promising approach.

## Acknowledgments

Funding received from Department of Biotechnology (DBT), Department of Science and Technology (DST), and Council of Scientific & Industrial Research (CSIR), Govt. of India are duly acknowledged. Fellowship support from Indian Institute of Technology Kharagpur is acknowledged by Mr. Saralasrita Mohanty.

## References

[1] J. Yang, J. Yu, Y. Cui, Y. Huang, New laser machining technology of $Al_2O_3$ ceramic with complex shape, Ceramics International 38 (2012) 3643–3648.
[2] J. Darsell, S. Bose, H.L. Hosick, A. Bandyopadhyay, From CT scan to ceramic bone graft, Journal of the American Ceramic Society 86 (2003) 1076–1080.
[3] J. Chevalier, L. Gremillard, Ceramics for medical applications: a picture for the next 20 years, Journal of the European Ceramic Society 29 (2009) 1245–1255.
[4] M.N. Rahaman, A. Yaoj, B.S. Bal, J.P. Garino, M.D. Ries, Ceramics for prosthetic hip and knee joint replacement, Journal of the American Ceramic Society 90 (2007) 1965–1988.
[5] S. Yang, H. Yang, X. Chi, J.R.G. Evans, I. Thompson, R.J. Cook, P. Robinson, Rapid prototyping of ceramic lattices for hard tissue scaffolds, Materials and Design 29 (2008) 1802–1809.
[6] S. Baskaran, G.D. Maupin, G.L. Gordon, Freeform fabrication of ceramics, American Ceramic Society Bulletin 77 (1998) 53–58.
[7] J.D. Cawley, Solid freeform fabrication of ceramics, Current Opinion in Solid State and Materials Science 4 (1999) 483–489.
[8] F. Filser, P. Kocher, F. Weible, H. Luthy, P. Sharer, L.J. Gauckler, Reliability and strength of all-ceramic dental restorations by direct ceramic machining (DCM), International Society of Computerized Dentistry 4 (2001) 89–106.
[9] S. Dhara, B. Su, Green machining to net shape alumina ceramics prepared using different processing routes, International Journal of Applied Ceramic Technology 2 (2005) 262–270.
[10] L. Yina, H.X. Penga, L. Yangb, B. Su, Fabrication of three-dimensional inter-connective porous ceramics via ceramic green machining and bonding, Journal of the European Ceramic Society 28 (2008) 531–537.
[11] B. Su, S. Dhara, L. Wang, Ceramic green machining: a top down approach for the rapid fabrication of complex shaped ceramics, Journal of the European Ceramic Society 28 (2008) 2109–2115.
[12] S. Dhara, P. Bhargava, Egg white as an environment friendly low cost binder for gelcasting of ceramics, Journal of the American Ceramic Society 84 (2001) 3048–3050.
[13] M.A. Janney, Method for Molding Ceramic Powders, US Patent no. 4894194, Jan. 16, 1990.
[14] M.A. Janney, O.O. Omatete, C.A. Walls, S.D. Nunn, R.J. Ogle, G. Westmoreland, Development of low-toxicity gelcasting systems, Journal of the American Ceramic Society 81 (1998) 581–591.
[15] S.D. Nunn, G.H. Kirby, Green machining of gelcast ceramic materials, Ceramic Engineering and Science Proceedings 17 (1996) 209–213.
[16] R.K. Kamboj, S. Dhara, P. Bhargava, Machining behavior of green gelcast ceramics, Journal of the European Ceramic Society 23 (2003) 1005–1011.
[17] B.K. Rhoney, A.J. Shih, R.O. Scattergood, J.L. Akemon, D.J. Gust, M. B. Grant, Wire electrical discharge machining of metal bond diamond wheels for ceramic grinding, International Journal of Machine Tools and Manufacture 42 (2002) 1355–1362.
[18] S. Mohanty, S. Dhara, A Process for Fabrication of Customized Ceramic Products by CNC Machining of Green Ceramics Compacts Using Diamond Impregnated Tool, Indian Patent 588/KOL/2012, May 2012.
[19] L.J.D. Oliveira, G.S. Bobrovnitchii, M. Filgueira, Processing and characterization of impregnated diamond cutting tools using ferrous metal matrix, International Journal of Refractory Metals and Hard Materials 25 (2007) 328–335.
[20] D.G. Lee, H.G. Lee, P.J. Kim, K.G. Bang, Micro-drilling of alumina green bodies with diamond grit abrasive micro-drills, International Journal of Machine Tools and Manufacture 43 (2003) 551–558.
[21] J. Konstanty, T.F. Stephenson, D. Tyrala, Novel Fe–Ni–Cu–Sn matrix materials for the manufacture of diamond-impregnated tools, Diamond Tooling Journal 3 (2011) 26.
[22] J. Konstanty, A. Romanski, New nanocrystalline matrix materials for sintered diamond tools, Materials Sciences and Applications 3 (2012) 779–783.
[23] Y. Li, H. Jiang, L. Pang, B. Wang, X. Liang, Novel application of nanocrystalline nickel electrodeposit: making good diamond tools easily, efficiently and economically, Surface and Coatings Technology 201 (2007) 5925–5930.
[24] S. Dhara, R.K. Kamboj, M. Pradhan, P. Bhargava, Shape forming of ceramics via gelcasting of aqueous particulate slurries, Bulletin of Materials Science 25 (2002) 565–568.
[25] S. Mohanty, A.P. Rameshbabu, S. Dhara, α-Alumina fiber with platelet morphology through wet spinning, Journal of the American Ceramic Society 95 (2012) 1234–1240.
[26] R.G. Munro, Evaluated material properties for a sintered α-alumina, Journal of the American Ceramic Society 80 (1997) 1919–1928.
[27] S.L. Fok, J. Smart, The accuracy of failure predictions based on weibull statistics, Journal of the European Ceramic Society 15 (1995) 905–908.
[28] D.J. Green, An Introduction to the Mechanical Properties of Ceramics, Cambridge University press, 285–307 (Chapter 9).